The incommensurate modulation of the structure of Sr2Nb2O7

Peter Daniels, Rafael Tamazyan, Christine A. Kuntscher, Martin Dressel, Frank Lichtenberg, Sander van Smaalen

Angaben zur Veröffentlichung / Publication details:

Daniels, Peter, Rafael Tamazyan, Christine A. Kuntscher, Martin Dressel, Frank Lichtenberg, and Sander van Smaalen. 2002. "The incommensurate modulation of the structure of Sr2Nb2O7." *Acta Crystallographica Section B Structural Science* 58 (6): 970–76. https://doi.org/10.1107/s010876810201741x.

Acta Crystallographica Section B
Structural Science
ISSN 0108-7681

The incommensurate modulation of the structure of $Sr_2Nb_2O_7$

Peter Daniels,[a]* Rafael Tamazyan,[a] Christine A. Kuntscher,[b] Martin Dressel,[b] Frank Lichtenberg[c] and Sander van Smaalen[a]

[a]Laboratory for Crystallography, Universität Bayreuth, D-95447 Bayreuth, Germany, [b]1 Physikalisches Institut, Universität Stuttgart, Pfaffenwaldring 57, D-70550 Stuttgart, Germany, and [c]Institut für Physik, EKM, Experimentalphysik VI, Universität Augsburg, Universitätsstr. 1, D-86135 Augsburg, Germany

Correspondence e-mail: peter.daniels@uni-bayreuth.de

Received 22 April 2002
Accepted 23 September 2002

The incommensurately modulated structure of $Sr_2Nb_2O_7$ at room temperature is reported, as determined by single-crystal X-ray diffraction. The crystal structure of $Sr_2Nb_2O_7$ comprises slabs with a perovskite-type structure that are separated by planes of additional O atoms. The driving force for the modulation is shown to be internal strain around the Sr atoms that lie at the interface between the slabs. At room temperature, $Sr_2Nb_2O_7$ crystallizes in the superspace group $Cmc2_1(\alpha 00)0s0$, with lattice parameters $a = 3.9544\,(7)$, $b = 26.767\,(6)$ and $c = 5.6961\,(8)$ Å. The modulation wave vector is determined as $\mathbf{q} = 0.488\,(3)\,\mathbf{a}^*$. X-ray diffraction data were collected at a synchrotron using a CCD area detector. A total of 3626 unique main reflections and 1262 unique first-order satellites with $I > 3\sigma(I)$ were obtained. Refinements using a single harmonic modulation wave converged at $R = 0.057$ ($R = 0.051$ for the main reflections and $R = 0.121$ for the satellite reflections). The modulated structure is interpreted in terms of rotations of NbO_6 octahedra and displacements of the Sr atoms.

1. Introduction

Recently, a group of compounds with the chemical composition $Sr_{1-y}La_yNbO_{3.5-x}$ have received much attention because of their electronic and dielectric properties (Kuntscher *et al.*, 2000; Lichtenberg *et al.*, 2001; Bobnar *et al.*, 2002). For the La-free end members of this group a variety of compounds with different oxygen content have been observed, leading to a homologous series with the chemical compositions $Sr_nNb_nO_{3n+2}$ (Williams *et al.*, 1993). The crystal structures are closely related to the perovskite structure type. Slabs of vertex-sharing NbO_6 octahedra are interrupted by planes containing additional O atoms (Ishizawa *et al.*, 1975; Schmalle *et al.*, 1995; Abrahams *et al.*, 1998; Elcoro *et al.*, 2001). Neighbouring slabs are shifted by $a/2$, resulting in a highly distorted coordination of the Sr atoms that are located between the slabs (Fig. 1). The width of slabs of NbO_6 octahedra can be measured by the number of octahedra between two interruption planes, and only two basic kinds of octahedral slabs, one with a width of four and one with a width of five octahedra, have been observed for strontium niobate so far. These slabs correspond to the $n = 4$ and $n = 5$ members of the homologous series, respectively. Other compositions consist of ordered or disordered mixtures of these two layer types (Williams *et al.*, 1993; Lichtenberg *et al.*, 2001).

The strontium niobate with the composition $Sr_2Nb_2O_7$ ($n = 4$) is ferroelectric below 1615 K (Ohi & Kojima, 1985). It is a candidate for the ferroelectric phase in non-volatile computer memories (Shoyama *et al.*, 1999). The basic crystal

structure has been determined by Ishizawa *et al.* (1975), who found it to have orthorhombic symmetry (space group $Cmc2_1$) with the reported cell dimensions $a = 3.933$, $b = 26.726$ and $c = 5.683$ Å (Fig. 1). Below 488 K, this compound develops an incommensurate modulation of its structure, producing satellite reflections at $0.490\mathbf{a}^*$ that have been observed in electron diffraction studies (Yamamoto *et al.*, 1980; Yamamoto, 1982). Here we report the results of a quantitative X-ray diffraction study of the incommensurately modulated structure of this compound at room temperature. It will be shown that the origin of the modulation is the resolution of the internal strain around the Sr atoms at the interface between perovskite-type slabs.

2. Experimental

Single crystals were prepared by the floating-zone method (Lichtenberg *et al.*, 2001). Since the crystal structure consists of layers of perovskite slabs, they exhibit a perfect cleavage along the direction of these planes, making the preparation of small single crystals that are suitable for X-ray diffraction experiments difficult. Several crystals were prepared by splitting and breaking them off a large sample block and gluing them to glass fibres. Subsequently the crystals were tested for their reflection profiles on a Nonius Mach3 diffractometer with a rotating-anode generator. Having found a suitable crystal with relatively narrow reflection profiles (less than 0.25° FWHM in ω scans) some of the satellite reflections could also be detected at their expected positions near $\mathbf{a}^*/2$. Their low intensities made the use of this diffractometer for data collection impossible, because the time needed for a complete and useful data set would have been unreasonably long. Precession photographs were recorded on image plates for the determination of the **q** vector. The satellite reflections could clearly be seen on photographs of $hk0$ layers (Fig. 2). Several profiles through strong satellites and neighbouring main reflections gave a **q** vector of $0.488\,(3)\,\mathbf{a}^*$, which closely corresponds to the value of 0.490 found by Yamamoto *et al.* (1980).

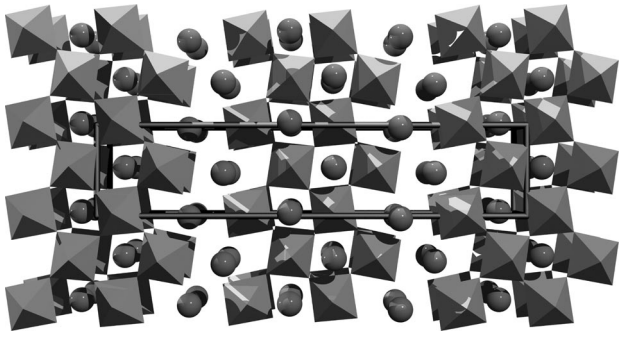

Figure 1
View along **a** of the basic crystal structure of $Sr_2Nb_2O_7$. NbO_6 octahedra are shown as light gray shaded octagons. Spheres represent the Sr atoms. The unit cell is outlined in black with **b** pointing from left to right and **c** pointing upwards. Neighbouring slabs are displaced by $\mathbf{a}/2$ with respect to each other.

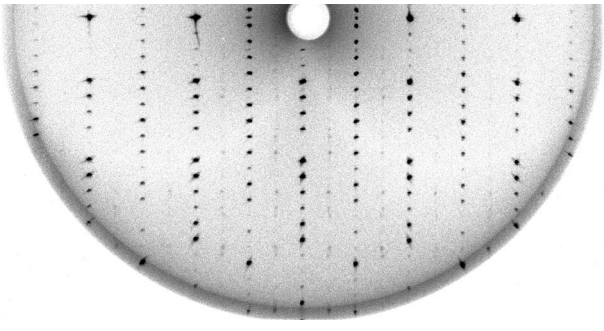

Figure 2
Precession photograph of an $hk0$ layer of $Sr_2Nb_2O_7$. Mo $K\alpha$ radiation, 40 kV, 30 mA, graphite monochromator, exposure time 16 h, recorded on an imaging plate.

The investigations using both a precession camera and a diffractometer verified the systematic extinctions found by Yamamoto (1982). The appearance of main reflections is in agreement with space group $Cmc2_1$, and the satellite reflections appear only for those main reflections allowed by this space group. The additional reflection condition $l + m = 2n$ for $h0lm$ leads to the superspace group $Cmc2_1(\alpha00)0s0$ (*International Tables for Crystallography*, 1999, Vol. C, 2nd ed., pp. 899–936). Only first-order satellites could be detected.

Subsequently, diffraction intensity data were recorded at the synchrotron beamline F1 of Hasylab at DESY (Hamburg, Germany), where a Huber diffractometer with Kappa geometry equipped with a CCD detector was used. Experimental details are listed in Table 1.[1] For the integration of intensities from the images, the commensurate approximation with a doubled a axis could be used because the **q** vector was close enough to $\mathbf{a}^*/2$ and because the C centring guaranteed that the satellites never approached each other closely. This commensurate approximation was the only way to obtain the intensities of satellites using the *SAINT* software (Bruker, 2000) available at the beamline.

The raw intensities were then corrected for absorption using the program *HABITUS* (Herrendorf, 1992). For this purpose, the crystal was assumed to be bounded by the forms {100}, {010} and {001}. Because of the perfect cleavage parallel to (010), these indices could easily be assigned to the large faces with the smallest separation (0.012 mm, see Table 1). The other two index triplets were chosen following a trial-and-error procedure, finally using the assignment giving the lowest internal residual ($R_{\rm int} = 6.91\%$). For all calculations, the program *JANA*2000 (Petricek & Dusek, 2000) was used.

3. Refinement

In all refinements, weighted structure amplitudes were used (see Table 1). In the first step, the average structure was refined using the main reflections only. This refinement

[1] Supplementary data for this paper are available from the IUCr electronic archives (Reference: CK0015). Services for accessing these data are described at the back of the journal.

Table 1
Experimental details.

Crystal data	
Chemical formula	$Sr_2Nb_2O_7$
Chemical formula weight	473
Cell setting, superspace group	Orthorhombic, $Cmc2_1(\alpha 00)0s0$
a, *b*, *c* (Å)	3.9544 (7), 26.767 (6), 5.6961 (8)
V (Å^3)	602.92 (19)
Z	4
D_x (Mg m^{-3})	5.21
Crystal size	0.120 × 0.070 × 0.012
Crystal colour	Colourless, transparent
Linear absorption coefficient (cm^{-1})	157.8
q	0.488(3)**a***
Data collection	
Radiation	Synchrotron
Wavelength (Å)	0.5
Diffractometer	IPDS Stoe
Detector	CCD: Bruker SMART1000
Temperature (K)	293
Range of *h*, *k*, *l*, *m*	$0 \rightarrow h \rightarrow 9$ $0 \rightarrow k \rightarrow 64$ $-13 \rightarrow l \rightarrow 9$ $-1 \rightarrow m \rightarrow 1$
No. of reflections	46577
No. of main reflections	23177
No. of satellites	23400
No. of satellites [$\sin(\theta)/\lambda \leq 0.8$]	6911
Unique main reflections	3723
Unique main reflections [$I > 3\sigma(I)$]	3626
Unique satellites	1403
Unique satellites [$I > 3\sigma(I)$]	1262
R_{int}	0.069
Absorption correction	Numerical
T_{min}	0.22
T_{max}	0.68
Refinement	
Refinement on	*F*
Criterion for observed reflections	$I > 3\sigma(I)$
Weighting scheme	$w = 1/[\sigma^2(\lvert F\rvert) + (0.02F)^2]$
Number of parameters used in refinement	105
R_{all} (observed/all)	0.057/0.059
R_{main} (observed/all)	0.051/0.053
$R_{satellites}$ (observed/all)	0.121/0.138
Goodness of fit (observed/all)	3.26/3.26

converged to $R = 5.8\%$, reproducing the positional parameters found by Ishizawa *et al.* (1975) to within three times their standard uncertainties (σ).

Checking the intensity distribution of the satellites revealed that for $\sin(\theta)/\lambda > 0.8$ all satellites were insignificantly weak. In order to avoid an unpredictable bias, these were omitted from all further calculations. Subsequently, in a trial-and-error process modulation, parameters for the various sites were introduced and refined. Several models of displacive modulations were tried in order to reproduce the intensities of the satellites. The best solution was obtained with a simple harmonic displacement of all atoms and an additional harmonic modulation of the temperature factor for Sr1 (Table 2 and supplementary material). The introduction of the latter improved R_{obs} from 6.90% to 5.65%. Using second and higher harmonics for the description of the modulation of positions and temperature factors did not improve the fit and led to a severe correlation between parameters and thus to unstable

Table 2
Refined parameters for $Sr_2Nb_2O_7$ (see also supplementary material).

The parameters B_x, A_y and A_z are the displacive modulation amplitudes along the axes *a*, *b* and *c*, respectively, where *A* refers to a sine and *B* to a cosine function.

Site	B_x (Å)	A_y (Å)	A_z (Å)
Sr1	0.0116 (10)	0.1266 (8)	0.0911 (7)
Sr2	0.0008 (7)	−0.0483 (7)	−0.0051 (7)
Nb1	0.0118 (7)	0.0134 (6)	0.0038 (6)
Nb2	0.0158 (7)	0.0099 (6)	0.0027 (6)
O1	−0.114 (7)	0.012 (6)	0.002 (5)
O2	−0.186 (8)	0.015 (7)	0.002 (6)
O3	0.000 (6)	−0.017 (6)	−0.181 (8)
O4	−0.067 (6)	0.048 (6)	0.014 (7)
O5	−0.098 (7)	−0.037 (7)	−0.018 (7)
O6	−0.066 (6)	0.001 (6)	0.008 (6)
O7	0.014 (6)	0.042 (6)	−0.167 (7)

refinements. The final *R* values were $R_{obs} = 5.65\%$ ($R_{all} = 5.94\%$) for all 5126 reflections, $R_{obs} = 5.13\%$ ($R_{all} = 5.28\%$) for the 3723 main reflections and $R_{obs} = 12.08\%$ ($R_{all} = 13.84\%$) for the 1403 satellites. R_{obs} refers to reflections with $I > 3\sigma(I)$. The results are listed in Table 2 and the supplementary material.

4. Discussion

The main contribution to the intensities of satellite reflections is produced by the deviation of the Sr atoms at the site Sr1 from their average position. The deviations from the lattice periodic average positions of the atoms as well as the variations of the distances between the atoms can be displayed in so-called *t*-plots (van Smaalen, 1995). The parameter *t* corresponds to a variation of the phase of the modulation. All atomic positions and distances that occur within a structure are found within one period [0,1] of *t*. Among the strongly scattering cations of this compound, the Sr1 site displays by far the largest modulation amplitudes (Table 2 and supplementary material, Fig. 3). Some O-atom positions have comparable amplitudes, but because of their relatively weak scattering factor the contribution to the satellite intensities is much less. This fact is responsible for the much larger standard uncertainties of the modulation amplitudes of O atoms compared with those of the cations (Table 2 and supplementary material).

The modulations are not restricted to a single direction or to a single atom site. While the Nb atoms remain almost fixed in their positions (Fig. 3), the O atoms move around them. Neither the Nb—O distances (Fig. 4) nor the O—Nb—O angles change significantly, but large modulations of the Nb—O—Nb angles are found (Fig. 5). The latter characterize the relative orientations of neighbouring NbO_6 octahedra. Hence, part of the modulation can be described as rotations of the NbO_6 octahedra. These rotations mainly occur about an axis parallel to the *b* axis (Fig. 6) as predicted by Yamamoto (1982). Valences as a function of *t* have been calculated by the bond-valence method using parameters given by Brese & O'Keeffe (1991). For Nb, a value of 5.0 is obtained, in accor-

dance with the formal valence of +5. The variations of the valences due to the modulation are within ±0.1 (Fig. 7*a*), which can be explained by the uncertainties in the bond lengths (Table 3) and by the fact that the parameters used for the calculations were determined for 'well behaved' periodic structures only (Brese & O'Keeffe, 1991).

The Sr2 site lies within the slabs with the perovskite-type structure. Its coordination sphere is a distorted version of the 12-fold coordination of the *A* cation in the perovskite-type structure (Fig. 8*a*). The variation due to the modulation of the individual Sr—O distances is much larger than that of the Nb—O distances (Fig. 4). However, these variations compensate each other such that the remaining *t* dependence of the valence of Sr2 is less than the uncertainties of the modulation model (Fig. 7*b*).

The Sr1 sites are at the boundaries of the slabs. In Fig. 1, the Sr1 atoms can alternately be assigned to the left and the right slabs. In this way, they could occupy ideal perovskite-like positions (Fig. 8*b*). The boundary between the slabs is then given by an empty plane of octahedra. The missing O atoms in this plane determine that the ideal perovskite-like positions have an 11-fold instead of a 12-fold coordination (Fig. 8*b*). Accordingly, the valence of an Sr atom at this position is calculated as 1.82, and Sr would be underbonded at this site. Therefore, the average positions of Sr1 atoms are shifted away from the ideal perovskite-like site by about 1.4 Å in the

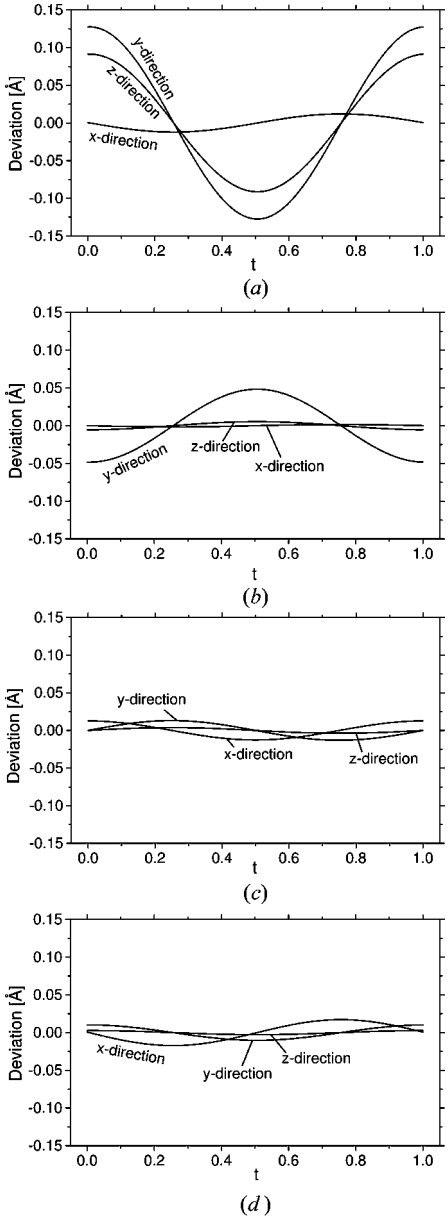

Figure 3
t-plot of the deviations from the average positions along the three crystal axes of the four cation sites: (*a*) Sr1; (*b*) Sr2; (*c*) Nb1; and (*d*) Nb2.

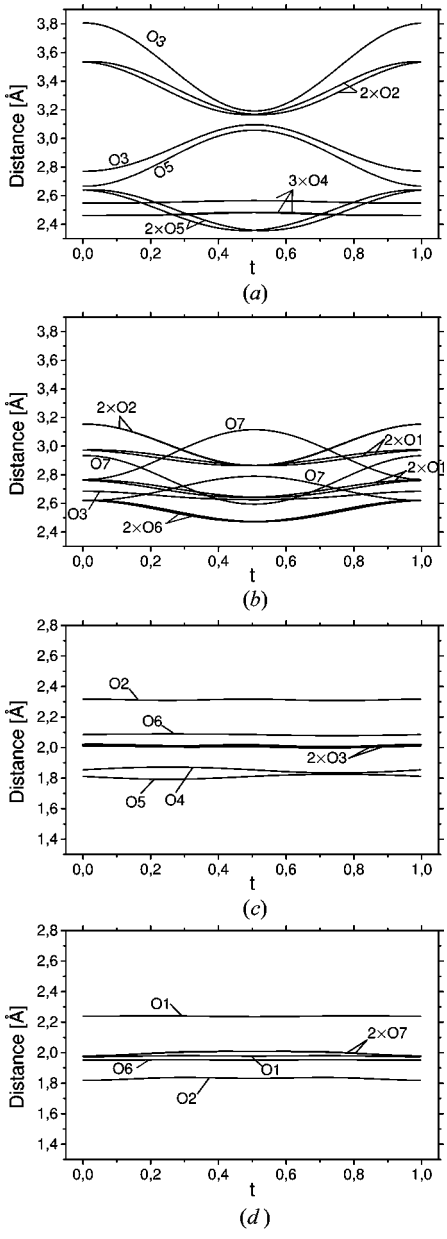

Figure 4
Distances between a metal atom and its surrounding O atoms plotted *versus t*: (*a*) Sr1; (*b*) Sr2; (*c*) Nb1; and (*d*) Nb2.

direction of the empty planes. Because neighbouring slabs are shifted by **a**/2 with respect to each other, there are two O atoms of the neighbouring slab relatively close to the average position of Sr1. This results in a tenfold coordination of Sr1 within a highly irregular coordination sphere. Although the longest among the ten shortest Sr1—O distances do not contribute significantly to the valence sum, they are considered as part of the coordination because they mark a step in the list of Sr1—O distances (Table 3) of more than 0.6 Å. The shortest Sr1—O distances are shorter than the Sr2—O distances in the perovskite-type environment (Fig. 4), resulting in the same computed valences for tenfold coordinated Sr1 and 12-fold coordinated Sr2 (Fig. 7).

We believe that the incommensurate modulation occurs to resolve the very short Sr—O distances of Sr1. The maximum deviation from the average position is found at $t = 0$ and $t = 0.5$ (Fig. 3). For these two t values, Sr1 has moved out of the square of the four nearest O atoms towards the other layer and towards the ideal perovskite position, respectively (Fig. 8). For $t = 0.5$ a maximum of the shortest Sr1—O distances is found, whereas for $t = 0$ a low secondary minimum occurs (Fig. 4). This results in a short average Sr1—O distance and consequently in the highest calculated valence (Fig. 7) for $t = 0$ and in a long average bond length and small calculated valence for $t = 0.5$. The modulation of the temperature factor for Sr1 is greatest for U_{22} and U_{33} (supplementary material). The two have a minimum at $t = 0$ and a maximum at $t = 0.5$, probably reflecting the variation in the average bond strength.

With the two extreme positions found for Sr1 avoiding the close neighbourhood of O4 and O5 forming a square (Fig. 8), one might expect a block-wave type of modulation, which allows only one of the two positions to be occupied. Although Yamamoto (1982) has explicitly excluded a discontinuous

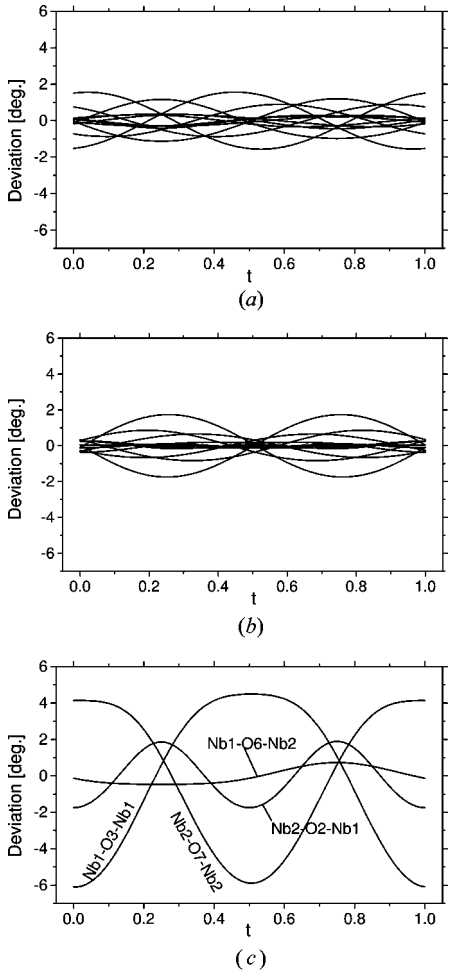

Figure 5
Deviations of the bond angles of NbO_6 octahedra from their values in the average structure plotted *versus* t: (*a*) O—Nb—O angles around Nb1; (*b*) O—Nb—O angles around Nb2; (*c*) Nb—O—Nb angles between vertex-sharing octahedra.

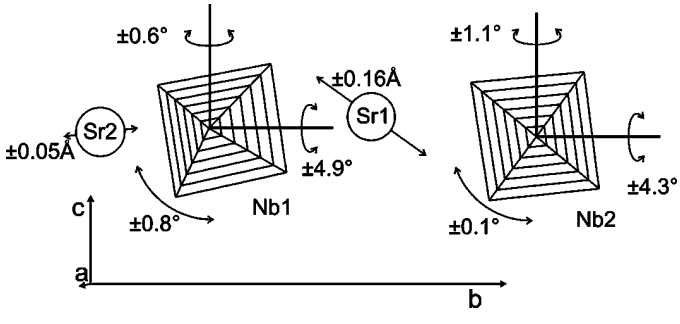

Figure 6
Rotation amplitudes of NbO_6 octahedra and displacements of the Sr atoms relative to the average structure.

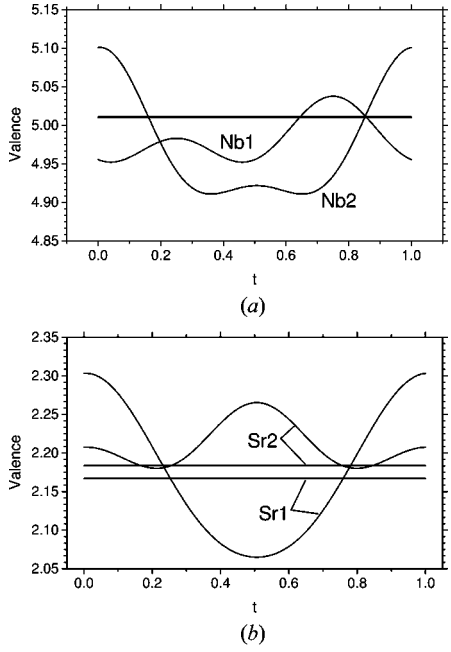

Figure 7
Valences of metal atoms as a function of the parameter t calculated from the metal- to O-atom distances by the bond-valence method. The horizontal lines give the valences for the basic structure. Parameters were $R^0_{Nb-O} = 1.911$ Å, $R^0_{Sr-O} = 2.118$ Å and $b = 0.37$ Å. The standard uncertainties due to those of the distances affect the second digit behind the decimal point. (*a*) Nb sites Nb1 and Nb2; (*b*) Sr sites Sr1 and Sr2. The valences for the two Nb sites in the basic structure coincide.

model for the modulation on the basis of symmetry arguments, a block-wave type of modulation can be in accordance with the superspace group and hence with the systematic extinctions. However, such behaviour can hardly be recognized from the final Fourier map (Fig. 9), and refinements using a block-wave function do not give a better fit to the data, whereas the introduction of additional modulation parameters leads to dependencies among them. The available data do not allow the determination of a more complex model. An electronic or magnetic origin for the modulation can be excluded because $Sr_2Nb_2O_7$ is a diamagnetic insulator.

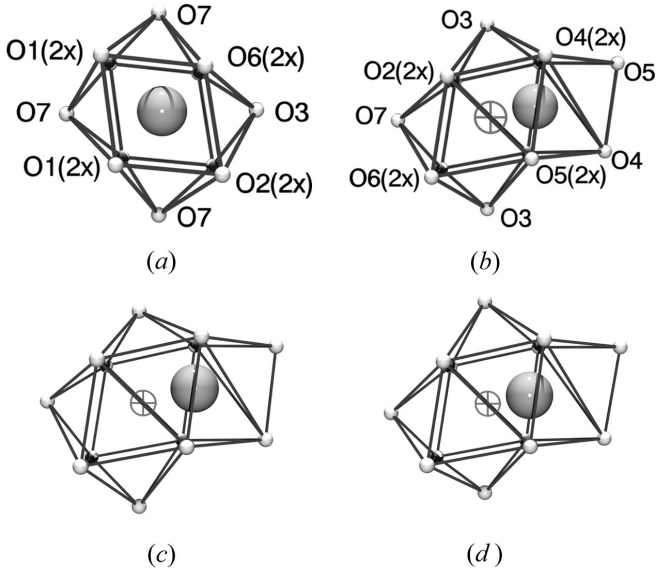

Figure 8
Coordination spheres of Sr1 and Sr2. The big spheres represent the Sr atoms while the smaller ones represent O atoms. The lines between O atoms are only meant to clarify the coordination geometries and do not represent chemical bonds. The symbol $\oplus$ marks the position that Sr1 would occupy in a 12-fold coordination that corresponds to the situation found for Sr2. (*a*) Sr2 coordination in the basic structure; (*b*) Sr1 coordination in the basic structure; (*c*) Sr1 coordination at $t = 0.0$; (*d*) Sr1 coordination at $t = 0.5$.

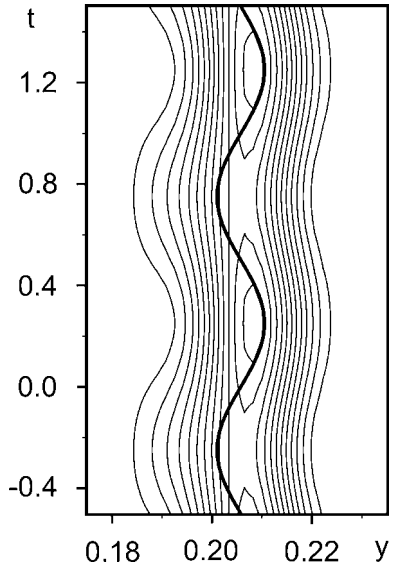

Figure 9
Section of the Fourier map (F_{obs}) in superspace at $x = 0.5$ and $z = 0.0298$, showing the component of the modulation function of Sr1 along **b**. The heavy line near the centre marks the calculated position of Sr1 in this section.

Table 3
Distances between metal atoms and O atoms in $Sr_2Nb_2O_7$.

The estimated standard uncertainties referring to the last digit given in parentheses for the maximum distances apply to the shortest distances as well. Seemingly duplicated lines give the distances for atom pairs that are symmetrically equivalent in the basic structure but are unequal in superspace.

First site	Second site	Basic	Average	Minimum	Maximum	Max − Min
Nb1	O5	1.808	1.809	1.803	1.813 (9)	0.010
Nb1	O4	1.853	1.854	1.834	1.872 (5)	0.039
Nb1	O3	2.005	2.009	2.001	2.019 (5)	0.017
Nb1	O3	2.005	2.009	2.001	2.019 (5)	0.017
Nb1	O6	2.084	2.084	2.069	2.098 (7)	0.029
Nb1	O2	2.309	2.313	2.308	2.317 (9)	0.010
Nb2	O2	1.825	1.829	1.807	1.843 (9)	0.036
Nb2	O6	1.952	1.952	1.951	1.953 (7)	0.002
Nb2	O1	1.975	1.977	1.960	1.991 (7)	0.031
Nb2	O7	1.994	1.997	1.979	2.009 (6)	0.030
Nb2	O7	1.994	1.997	1.979	2.009 (6)	0.030
Nb2	O1	2.237	2.239	2.235	2.241 (7)	0.006
Sr1	O4	2.467	2.470	2.461	2.484 (6)	0.023
Sr1	O4	2.467	2.470	2.461	2.484 (6)	0.023
Sr1	O5	2.497	2.500	2.479	2.522 (6)	0.042
Sr1	O5	2.497	2.500	2.479	2.522 (6)	0.042
Sr1	O4	2.553	2.556	2.548	2.566 (8)	0.018
Sr1	O5	2.862	2.863	2.667	3.058 (9)	0.391
Sr1	O3	2.922	2.928	2.771	3.096 (9)	0.325
Sr1	O2	3.384	3.350	3.167	3.536 (7)	0.370
Sr1	O2	3.384	3.350	3.167	3.536 (7)	0.370
Sr1	O3	3.499	3.499	3.192	3.806 (9)	0.614
Sr1	O6	4.144	4.146	4.041	4.253 (5)	0.212
Sr1	O6	4.144	4.146	4.041	4.253 (5)	0.212
Sr1	O7	4.220	4.220	4.145	4.296 (7)	0.151
Sr1	O3	4.323	4.326	4.213	4.435 (5)	0.223
Sr1	O3	4.323	4.326	4.213	4.435 (5)	0.223
Sr2	O6	2.547	2.548	2.520	2.576 (6)	0.055
Sr2	O6	2.547	2.548	2.520	2.576 (6)	0.055
Sr2	O3	2.650	2.653	2.626	2.685 (5)	0.058
Sr2	O1	2.700	2.701	2.642	2.762 (6)	0.120
Sr2	O1	2.700	2.701	2.642	2.762 (6)	0.120
Sr2	O7	2.700	2.702	2.620	2.790 (7)	0.170
Sr2	O7	2.763	2.764	2.595	2.934 (9)	0.339
Sr2	O1	2.917	2.917	2.816	3.019 (6)	0.203
Sr2	O1	2.917	2.917	2.816	3.019 (6)	0.203
Sr2	O7	2.940	2.940	2.766	3.115 (9)	0.349
Sr2	O2	3.006	3.008	2.864	3.154 (7)	0.289
Sr2	O2	3.006	3.008	2.864	3.154 (7)	0.289

Carsten Paulmann is thanked for his assistance with the synchrotron experiment. Beam time at beamline F1 of Hasylab at DESY (Hamburg, Germany) was obtained under proposal number II-00-029. We gratefully acknowledge financial support by the German Science Foundation (DFG).

References

Abrahams, S. C., Schmalle, H. W., Williams, T., Reller, A., Lichtenberg, F., Widmer, D., Bednorz, J. G., Spreiter, R., Bosshard, Ch. & Günter, P. (1998). *Acta Cryst.* B**54**, 399–416.
Bobnar, V., Lunkenheimer, P., Hemberger, J., Loidl, A., Lichtenberg, F. & Mannhart, J. (2002). *Phys. Rev. B*, **65**, 155115-1–155115-8.

Brese, N. E. & O'Keeffe, M. (1991). *Acta Cryst.* B**47**, 192–197.
Bruker (2000). *SAINT. Program for the Integration of Intensities from Diffraction Images.* Bruker AXS GmbH, Karlsruhe, Germany.
Elcoro, L., Perez-Mato, J. M. & Withers, R. L. (2001). *Acta Cryst.* B**57**, 471–484.
Herrendorf, W. (1992). PhD thesis, University of Karlsruhe, Germany.
Ishizawa, N., Marumo, F., Kawamura, T. & Kimura, M. (1975). *Acta Cryst.* B**31**, 1912–1915.
Kuntscher, C. A., Gerhold, S., Nücker, N., Cummins, T. R., Lu, D.-H., Schuppler, S., Gopinath, C. S., Lichtenberg, F., Mannhart, J. & Bohnen, K.-P. (2000). *Phys. Rev. B*, **61**, 1876–1883.
Lichtenberg, F., Herrnberger, A., Wiedenmann, K. & Mannhart, J. (2001). *Prog. Solid State Chem.* **29**, 1–70.
Ohi, K. & Kojima, S. (1985). *Jpn. J. Appl. Phys.* **24**, Suppl. 24–2, 817–819.
Petricek, V. & Dusek, M. (2000). *The Crystallographic Computing System JANA*2000. Institute of Physics, Praha, Czech Republic.
Schmalle, H. W., Williams, T., Reller, A., Lichtenberg, F., Widmer, D. & Bednorz, J. G. (1995). *Acta Cryst.* C**51**, 1243–1246.
Shoyama, M., Tsusuki, A., Kato, K. & Murayama, N. (1999). *Appl. Phys. Lett.* **75**, 561–562.
Smaalen, S. van (1995). *Cryst. Rev.* **4**, 79–202.
Williams, T., Lichtenberg, F., Widmer, D., Bednorz, J. G. & Reller, A. (1993). *J. Solid State Chem.* **103**, 375–386.
Yamamoto, N. (1982). *Acta Cryst.* A**38**, 780–789.
Yamamoto, N., Yagi, K., Honjo, G., Kimura, M. & Kawamura, T. (1980). *J. Phys. Soc. Jpn*, **48**, 185–191.